Proposal for study of charm component in the nucleon via J/ψ measurement with the J-PARC E16 spectrometer

Y. Morino(*Spokesperson*)[1], K. Aoki[1], D. Arimizu[2], S. Asamizu[4], S. Ashikaga[2], W.-C. Chang[3], T. Chujo[4], H. En'yo[5], S. Esumi[4], H. Hamagaki[6], R. Honda[1], M. Ichikawa[2], K. Kanno[5], S. Kajikawa[13], A. Kiyomichi[8], S. Kyan[4], C.-H. Lin[3], C.-S. Lin[3], H. Murakami[7], T. N. Murakami[7], R. Muto[1], W. Nakai[5], S. Nakasuga[2], M. Naruki[2], H. Noumi[9], K. Ozawa[1], T. Sakaguchi[10], H. Sako[11], S. Sato[11], F. Sakuma[5], S. Sawada[1], M. Sekimoto[5], K. Shigaki[12], K. Shirotori[9], H. Sugimura[1], K. N. Suzuki[2], T. N. Takahashi[5], K. Yamaguchi[2], and S. Yokkaichi[5]

[1]KEK, High Energy Accelerator Research Organization, Tsukuba, Ibaraki 305-0801, Japan
[2]Department of Physics, Kyoto University, Kyoto 606-8502, Japan
[3]Institute of Physics, Academia Sinica, Taipei 11529, Taiwan
[4]Center for Integrated Research in Fundamental Science and Engineering, University of Tsukuba, Tsukuba, Ibaraki 305-8577, Japan
[5]RIKEN, Wako, Saitama 351-0198, Japan
[6]Department of Engineering, Nagasaki Institute of Applied Science, Nagasaki, Nagasaki 851-0193, Japan
[7]Department of physics, University of Tokyo, 7-3-1 Hongo, Tokyo 113-0033, Japan
[8]Japan Synchrotron Radiation Research Institute (JASRI), 1-1-1 Koto, Sayo, Hyogo 679-5198, Japan
[9]Research Center for Nuclear Physics (RCNP), Osaka University, 10-1 Mihogaoka, Ibaraki, Osaka, 567-0047, Japan
[10]Physics Department, Brookhaven National Laboratory, Upton, NY 11973-5000, USA

[11]Advanced Science Research Center, Japan Atomic Energy Agency,
Tokai, Ibaraki 319-1195, Japan
[12]Graduate School of Science, Hiroshima University,
Higashi-Hiroshima, Hiroshima 739-8526, Japan
[13]Department of Physics, Tohoku University, Sendai, 980-8578, Japan

December 19, 2021

Executive Summary

The existence of $|uudc\bar{c}\rangle$ Fock components in a nucleon, which is called *"intrinsic charm"*, has been suggested in the early 1980's[1]. The intrinsic charm tends to have a large momentum fraction (x), unlikely *"extrinsic charm"* which is generated by gluon splitting perturbatively. Parton distribution function (PDF) of the intrinsic charm can be different from the PDF of intrinsic anti-charm. These features of the intrinsic charm have been applied for possible solutions of various unexpected phenomena related to heavy quarks. However, the existence of the intrinsic charm remains still inconclusive, despite several experimental and theoretical studies to evaluate the probability of the intrinsic charm.

Identification of a clean and characteristic phenomenon of the intrinsic charm will be a smoking gun. The anomalous J/ψ suppression of the yield per nucleon at large x_F in high energy hadron-nucleus collisions is one of the most striking phenomena related to the intrinsic charm[4]. An introduction of *"soft"* production of J/ψ due to the intrinsic charm can account for the anomalous J/ψ suppression intutively[8]. On the other hand, the energy loss model, which assumes the color singlet model for J/ψ production and the large energy loss for the color-octet $c\bar{c}$ pair in the nuclear matter, can also explain the anomalous suppression[46]. Since it is difficult to reject the energy loss model from the experimental results to date, the present J/ψ suppression cannot be regarded as clear evidence of the intrinsic charm.

The energy loss effect of the $c\bar{c}$ color-octet production becomes negligible in the case of backward production in low energy collisions, since the path length of the color-octet becomes significantly short. On the other hand, the intrinsic charm scenario predicts J/ψ suppression at backward regions in a similar way to the forward J/ψ suppression. Therefore, backward J/ψ suppression in low energy collisions is the characteristic phenomenon of the intrinsic charm. The measurement of backward J/ψ production in low energy hadron-nucleus collisions will provide crucial information to judge the origin of the observed J/ψ suppression, that is, the intrinsic charm or the energy loss.

A measurement of backward J/ψ production in low energy hadron-nucleus collisions can be performed as a by-production of the J-PARC E16 experiment[39]. The energy of the proton beam at the high momentum beam line (30 GeV) is significantly lower than previous measurements of J/ψ suppression, which are several hundred GeV. The cross section of J/ψ via the hard processes gets considerably small in the case of low energy collisions. It leads that the fraction of the contribution from the intrinsic charm increases and backward J/ψ production gets to be more sensitive to the intrinsic charm. The effect of the intrinsic charm will emerge as the difference of α for J/ψ ($\sigma_A = \sigma_N \times A^\alpha$) between mid-rapidity and backward.

Although the original E16 experiment is really suitable for measuring the backward J/ψ production, the experiment cannot measure the mid-rapidity production due to the acceptance. Therefore, an experiment is proposed to cope with the inefficiency for J/ψ at $x_F \sim 0$ in this proposal. The targets are moved upstream by 26 cm near a vacuum window of a beam pipe. The planned targets are 400 μm C and 200 μm Pb. Since the interaction length of the targets is the same as the original E16 experiment, the event rate of this experiment is within the capability of the E16 spectrometer. We

request 1200 hours (50 days) beamtime with the proposed setup to confirm the effect of the intrinsic charm, after the RUN1 data taking of the E16 experiment is completed.

Table 1: Summary of beam time request.

beamline	high-p beamline
beam intensity	10^{10} ppp
beam particle	proton
beam energy	30 GeV
shift	1200 hours (50days)

1 Introduction

1.1 Intrinsic charm

The existence of $|uudc\bar{c}\rangle$ Fock components in a proton, which is called *"intrinsic charm"*, has been suggested in the early 1980's[1, 2]. The intrinsic charm was introduced to account for the unexpected large cross section of charm in forward regions at first.

The intrinsic charm has two significant features as follows. The intrinsic charm tends to have a large momentum fraction (x), unlikely *"extrinsic charm"* which is generated by gluon splitting perturbatively. Second, parton distribution function (PDF) of the intrinsic charm can be different from the PDF of intrinsic anti-charm. These features of the intrinsic charm have been applied for possible solutions of various unexpected phenomena related with heavy quarks:*e.g.,* anomalous J/ψ suppression at large Feynman-x (x_F) regions in hadron-nucleus collisions[3, 4, 5, 6, 7, 8], asymmetries between leading and non-leading charm hadro-production[9, 10, 11, 12, 13], anomalous large branching ratio of J/$\psi \to \rho\pi$ decay[14, 15], and hadro-production of double J/ψ at large x_F regions[16, 17, 18, 19]. Since the intrinsic charm enables non-perturbative charm production, the cross section of charm will increase from the perturbative calculation especially at low energy regions. This topic is closely related to possible experiments about heavy quarks at J-PARC. The intrinsic charm becomes an essential topic for not only hadron physics but also particle physics since the precise determination of PDF is crucial for the interpretation of measurements at high energy hadron colliders. It has been pointed out that the intrinsic charm is relevant to various interesting studies such as Higgs production, Z-boson production, single-top production, and dark matter searches [20, 21, 22, 23, 24]. The confirmation and the quantitative evaluation of the intrinsic charm is an important baseline for the development of physics.

Despite several experimental and theoretical studies to evaluate the probability of the intrinsic charm in a proton (P_{IC}), even the existence of the intrinsic charm remains inconclusive. P_{IC} was initially suggested to be $\sim 1\%$[1]. $P_{IC} \sim 0.5\%$ was theoretically predicted by a chiral quark model[25]. Recently, P_{IC} was also calculated by lattice QCD, and their results were compatible with the result of the chiral quark model[26, 27, 28]. Experimentally, a straight and direct way to study the intrinsic charm is a measurement of the charm structure function from deep inelastic scattering. The charm structure function at large-x regions measured by EMC provided the positive result for the presence of the intrinsic charm[29]. P_{IC} evaluated from EMC data was $0.3 \sim 0.9\%$ depending on the used models[30, 31, 32]. The global analyses of the proton PDF with the intrinsic charm contribution were also carried out by several authors[33, 34, 35, 36]. However, there is a significant tension between HERA[37] and EMC data in regions of overlapping kinematics. The results of the global analyses strongly depend on the choice of input data sets and the treatment of the tension: varing from $P_{IC} \leq\sim 0.2\%$ at the 5σ level to $P_{IC} \sim 4\%$. The current status of the P_{IC} analyses is reviewed in Ref.[38]. In summary, the existence of the intrinsic charm is neither rejected nor confirmed and P_{IC} seems to be less than a few % levels even if it exists.

It is obvious that additional experimental results are necessary to the confirmation

and the quantitative evaluation of the intrinsic charm. One of the solutions to this situation is to perform a precise measurement of the charm structure function at large-x regions, which could be carried out at the future electron-ion collider. Another way is an identification of a characteristic phenomenon of the intrinsic charm by a measurement of observables to be sensitive to the large-x charm component. Backward J/ψ production in low energy proton-nucleus collisions is a sensitive and clean observable to the existence of the intrinsic charm. The effect of the intrinsic charm will emerge as the J/ψ suppression of the yield per nucleon at backward regions.

1.2 J/ψ suppression at large x_F in hadron-nucleus collisions

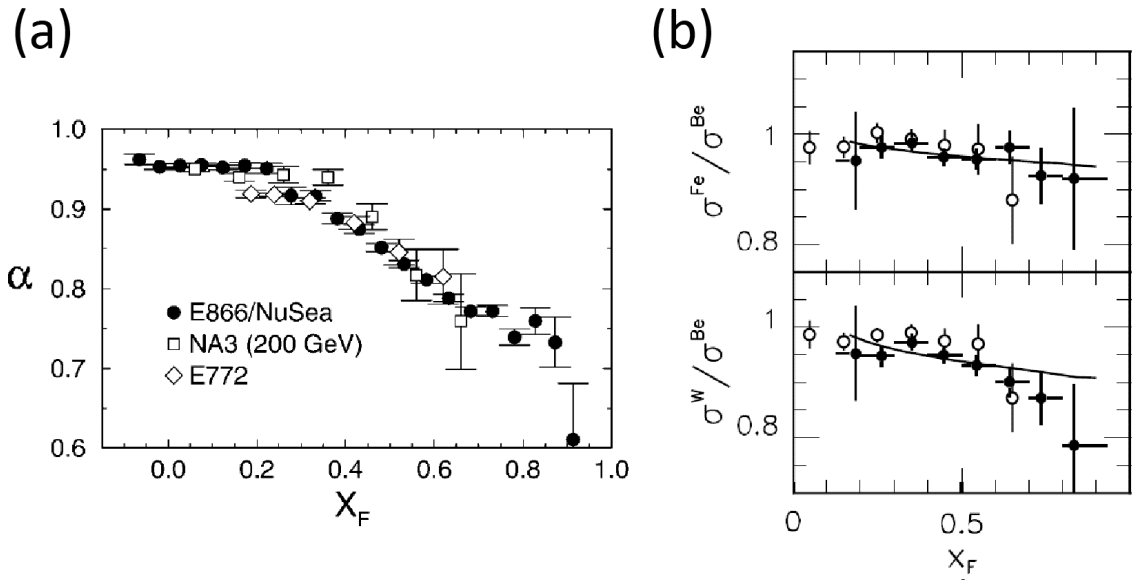

Figure 1: (a): α for J/ψ as a function of x_F from E866 (solid circles), E772 (diamonds), and NA3 (open squares)[4]. α is defined by $\sigma_A = \sigma_N \times A^\alpha$. (b): Ratios of the dimuon yield from Drell-Yan process per nucleon for Fe/Be (Top) and W/Be (Bottom) as a function of x_F from E772 (open circles) and E866 (solid circles)[42].

Several experiments have reported the anomalous J/ψ suppression of the yield per nucleon at large x_F in hadron-nucleus collisions[4, 3, 6, 7, 5]. Figure 1(a) shows the dependence of the J/ψ cross section on a nuclear number (A) in terms of α as a function of x_F measured at E866, E772, and NA3[4, 3, 5]. α is defined by $\sigma_A = \sigma_N \times A^\alpha$, where σ_N is the cross section on a nucleon. α is close to 1 at $x_F <\sim 0.3$, which indicates that J/ψ is produced by hard processes and interaction between J/ψ and the nuclear matter is not strong. It is consistent with the typical picture for a heavy quarkonium. However, α decreases to $\sim 2/3$ as x_F becomes larger, which means J/ψ production is strongly suppressed by the nuclear matter. When J/ψ is considered to be produced by the hard processes conventionally, this suppression pattern indicates only forward J/ψ strongly interacts with the nuclear matter. These results are surprising since they contradict the

picture of color transparency due to the smallness of heavy quarkonium. In addition, the x_F dependence of the J/ψ suppression also contradicts pQCD factorization[41]. On the other hand, Fig. 1(b) shows ratios of the dimuon yield from Drell-Yan process per nucleon for Fe/Be (Top) and W/Be (Bottom) as a function of x_F at E772 and E866[42]. α for the Drell-Yan dumon is still ~ 0.95 at the most forward region. Therefore, the J/ψ suppression cannot be interrupted as the result of nuclear shadowing and/or initial parton energy loss. Some specific effects for the heavy quarkonium must be considered. Two scenarios resolve this puzzle of the J/ψ suppression in hadron-nucleus collisions.

One of the solutions for the J/ψ suppression puzzle is an introduction of *"soft"* production of J/ψ due to the intrinsic charm[8, 43]. It assumes the following process. The intrinsic charm Fock state ($|uudc\bar{c}\rangle$) emerges in the incident proton ($|u\bar{d}c\bar{c}\rangle$ in the case of the π^+ beam). The light quark components in the incident proton interact with soft gluons emitted from the nuclear surface. The remaining $c\bar{c}$ pair hadronizes to quarkonium and passes through the nucleus due to their smallness. This process is almost occurred on the nuclear surface, leading to an approximate $A^{2/3}$ dependence. Figure 2(a) shows a conceptual view of the above process. The intrinsic charm must carry a large fraction of the longitudinal momentum of the incident proton in order to minimize the off-shell component of the proton with the large mass of charm. Therefore, J/ψ generated via the soft process tends to have large x_F, while the yield of J/ψ generated via the hard processes decreases rapidly with x_F. It can explain the J/ψ suppression pattern, that is, the intrinsic charm contribution becomes dominant for J/ψ production, and then α approaches 2/3 as x_F increases.

The other solution for the J/ψ suppression puzzle is an energy loss model of J/ψ[44, 45, 46]. Fig. 2(c) shows a conceptual view of the energy loss model. The most important assumption in the model is that a $c\bar{c}$ pair is produced in a color octet state via the hard processes and then hadronizes to J/ψ after the hadronization time (τ_ψ) in the rest frame of the $c\bar{c}$ pair. The $c\bar{c}$ pair remains the color octet state and interacts strongly with the nuclear matter until it hadronizes. Since a path length of the color octet state is proportional to its $\beta\gamma$, the fast $c\bar{c}$ pair loses its energy significantly enough to explain the suppression pattern. The energy loss model almost reproduces the J/ψ suppression pattern of the past measurements[46]. Since it is difficult to reject the energy loss model from the experimental results to date, the present J/ψ suppression cannot be regarded as evidence of the intrinsic charm. Indeed, there is also a possibility that the J/ψ suppression pattern is the result of the combination of the intrinsic charm and the energy loss.

The measurement of backward J/ψ production in low energy hadron-nucleus collisions is attractive to break through this situation. The energy loss of the $c\bar{c}$ color octet gets smaller in the case of backward production in low energy collisions, since the path length of the color octet becomes short due to its small β as shown in Fig. 2(d). On the other hand, the interaction between the intrinsic charm state ($|uudc\bar{c}\rangle$ or $|uddc\bar{c}\rangle$) emerged in the nucleon on the surface of the target and the incident proton produces backward J/ψ in a similar way to forward J/ψ production via the intrinsic charm (Fig. 2(b)). The contribution from the intrinsic charm is also expected to be almost independent of the collision energy[47]. When x_F of J/ψ gets close to -1 and the $c\bar{c}$ pair is sufficiently slow, the energy loss can be neglected while the effect of

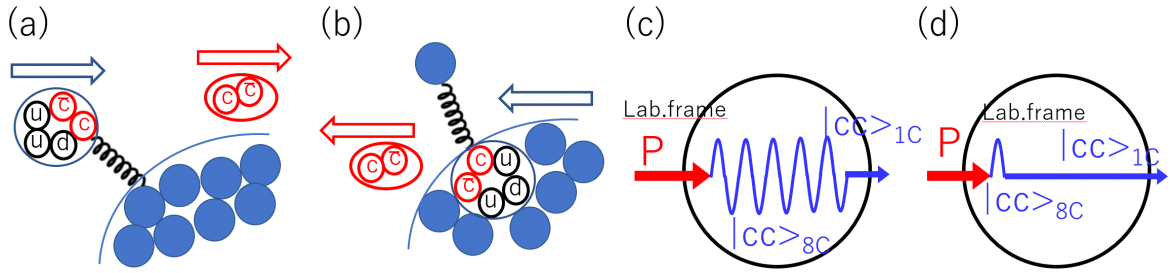

Figure 2: Conceptual views of the two interpretations of the J/ψ suppression: (a) forward J/ψ production via the intrinsic charm, (b) backward J/ψ production via the intrinsic charm, (c) energy loss of the color octet in the case of forward production, and (d) energy loss of the color octet in the case of backward production.

J/ψ production via the intrinsic charm will remain. Furthermore, the cross section of J/ψ via the hard processes gets considerably small in the case of low energy collisions. It leads that the fraction of the contribution from the intrinsic charm increases and backward J/ψ production gets to be more sensitive to the intrinsic charm. The measurement of backward J/ψ production in low energy hadron-nucleus collisions can be expected to be a good probe for the existence of the intrinsic charm. Such measurements have not been carried out yet. So far, the most backward measurement of J/ψ production ($x_F >\sim -0.3$) was carried out by HERA-B[6]. However, J/ψ production via the intrinsic charm is expected to appear at more backward regions and the $c\bar{c}$ pair is not sufficiently slow due to the high energy of the incident proton beam at HERA-B (920 GeV). In this proposal, we propose a new measurement of backward J/ψ production to confirm the intrinsic charm by using a 30 GeV proton beam at the J-PARC high momentum beamline and the J-PARC E16 spectrometer[39].

2 Experiment

2.1 Detector Setup

The measurement of backward J/ψ production in low energy hadron-nucleus collisions can be performed at the Hadron Experimental Facility at J-PARC. The measurement requires that an incident beam has enough energy to produce J/ψ and a beam intensity is high enough to compensate for the small cross section of J/ψ at low energy regions (nb order). The detectors for the measurement must have acceptance for backward J/ψ production, that is, a lepton spectrometer with large acceptance for backward scattering and high rate tolerance is suitable. A few experimental targets from light to heavy nuclei are necessary to measure the nuclear dependence of the J/ψ yield.

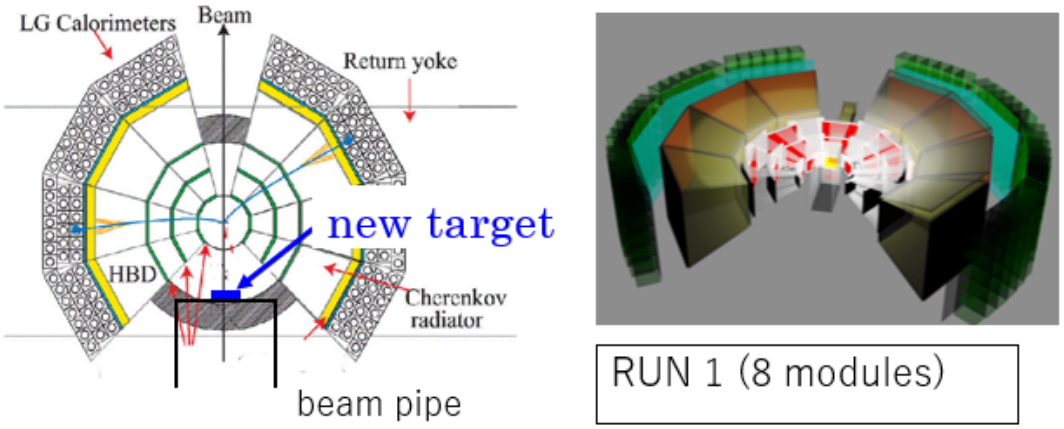

Figure 3: The schematic view of the RUN1 E16 spectrometer: (Left) the plan view. The new experimental target is also shown, (Right) the 3D view .

The J-PARC E16 spectrometer satisfies the requirements for the backward J/ψ measurement. The E16 experiment was proposed to perform a systematic study for the mass modification of light vector meson (ϕ and ω). While the E16 spectrometer consists of 26 detector modules in the case of the full installation, the first physics RUN (call as "RUN1") will be carried out by the spectrometer with 8 modules. The budget of the spectrometer for the RUN1 has been secured. The experiment of this proposal is also supposed to be performed with the spectrometer with 8 modules. The schematic view of the E16 spectrometer at the RUN1 is shown in Figure 3.

Although the original E16 experiment is really suitable for measuring backward J/ψ production, the experiment cannot measure J/ψ production at mid-rapidity due to the acceptance. Since the effect of the intrinsic charm will emerge as the difference of α for J/ψ ($\sigma_A = \sigma_N \times A^{\alpha}$) between mid-rapidity and backward, the measurement of the mid-rapidity J/ψ production is also indispensable. Therefore, we propose the experiment with new targets which are moved upstream by 26 cm near a vacuum window of a beam pipe to cope with the inefficiency for mid-rapidity J/ψ production. The new

experimental target is shown in Fig. 3. Upgrades of the E16 spectrometer are not necessary. Since the heavy nucleus is advantageous to study the nuclear dependence,

Table 2: Summary of the planned experimental target.

	targets
E16 experiment(RUN1)	400 μm C, 100 μm Ti, 160 μm Cu
This experiment	400 μm C, 100 μm Ti, 200 μm Pb

the Pb target (100μm$\times$2) is selected. Planned experimental targets are summarized at Table. 2. The vacuum window of the beam pipe can be utilized as the experimental target. 100 μm Ti at Table. 2 corresponds to the vacuum window. The total interaction length of the targets is $\sim$0.2%, which is the same as the E16 RUN1. While the number of charged particles emitting by a p+Pb collision is nearly three times higher than that of a p+Cu collision, the distance between the target and the innermost detector is nearly three times as long in the setup of this experiment. The E16 spectrometer is enable to deal with the event rate of this experiment.

2.2 Trigger

A coincidental hit of a HBD segment and a LG block located just behind the segment is required with a corresponding hit on the most-outer GTR to trigger an electron track candidate in the E16 experiment. The E16 trigger requires two electron candidates who have an opening angle of larger than a threshold. Basically, the same trigger logic can be used in this experiment, while the detail of the trigger condition must be optimized for this experiments.

Electron pair candidates who have the certain opening angle will increase by moving the targets and using the Pb target. On the other hand, since electrons from J/ψ have significantly higher energy than the background electrons from π^0, a requirement of a high energy deposit at the LG block for the trigger is effective to suppress the trigger rate without reducing the efficiency. From Monte-Carlo study described in [61], the threshold of the LG hit for electron energy of 0.7 GeV is enough to reduce the trigger rate to less than 500 Hz without reducing the efficiency. However, in this Monte-Carlo study, only contributions from the targets were considered. In addition, the time structure of the proton beam in the high-p beamline was not also considered.

The pilot run of the E16 experiment has been carried out. The pilot run can also be considered the pilot run of the proposed experiment. The trigger rate of the E16 pilot run was higher than expected. The reason of the high trigger rate is still under analysis and is not yet understood fully. Under such circumstances, it is difficult to estimate the reliable trigger rate at present from the simulation study. This time, we will estimate the rough rate from the actual trigger rate and show the live time based on the actual timing information of the trigger request. Figure 4 shows the trigger rate as a function of the LG threshold. This plot is based on the result of the E16 pilot run. The measured LG threshold dependence of the trigger rate was scaled by the measured trigger rate with the final configuration of the pilot run. The electron

energy of 0.7 GeV corresponds to about 140 mV at the LG threshold in Fig. 4 and the corresponding trigger rate is about 650 Hz. This proposal assumes the trigger rate of 1 kHz conservatively.

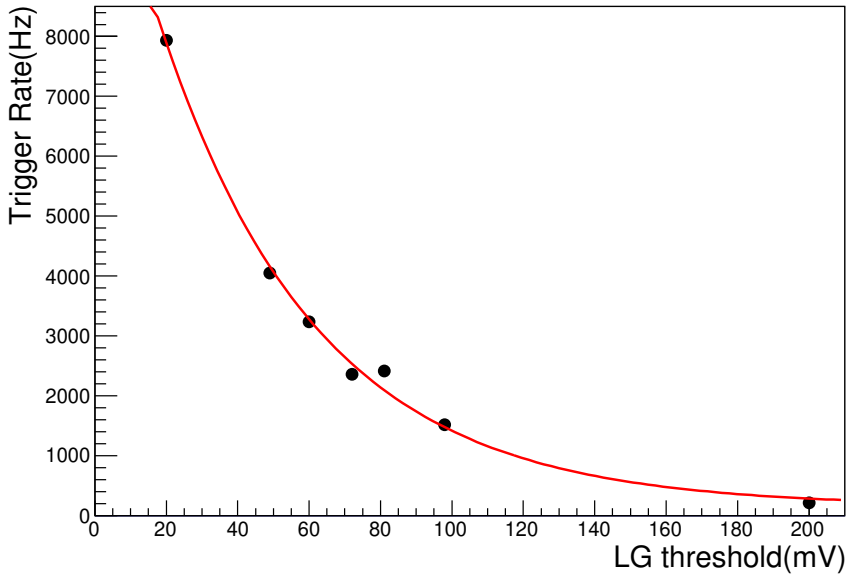

Figure 4: The E16 trigger rate as a function of the LG threshold.

The pilot run revealed that the proton beam in the high-p beamline had a significant time structure. The time structure affects the DAQ livetime strongly and may increase the trigger rate itself. The DAQ live time is estimated from the actual seamless tdc data of the trigger request. The E16 DAQ for RUN1 will have a dead time of about 80 μsec and will have an APV buffer for one event. Assuming the fixed dead time of 100 μsec and the one event buffer, the DAQ live time is evaluated from the tdc data of the pilot run at the 1 kHz trigger rate. The result is about 60% and we assume it in this proposal. As already explained, the live time depends strongly on the time structure of the proton beam as well as the trigger rate. The time structure is expected to be improved by updating the power supply of the Main Ring during the long shutdown and adopting new optics at the hadron beamline. The effect cannot be estimated at present and it will be clarified with the trigger rate by the time the TDR is submitted.

3 Results

3.1 Simulation Study

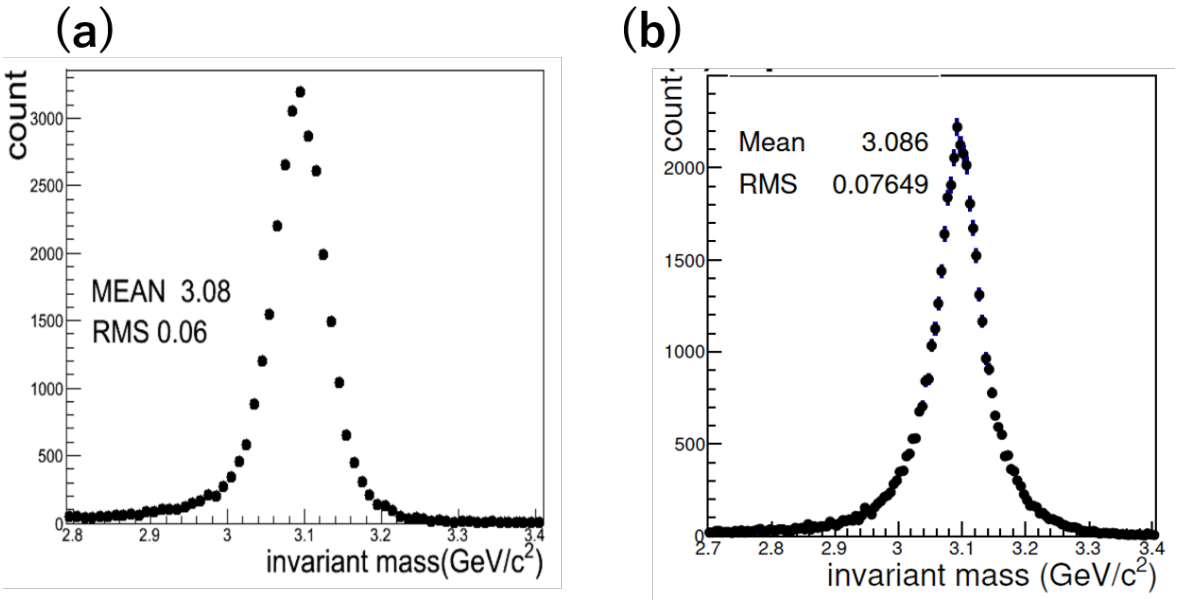

Figure 5: The simulated invariant mass distributions for the reconstructed J/ψ: (a) the E16 RUN1 and (b) this experiment.

A full detector Monte-Carlo simulation based on GEANT4 packages was performed to evaluate the feasibility of the proposed study. The E16 RUN1 configuration of 8 modules was assumed in this study. The LG response in the simulation was roughly tuned based on the achieved detector performance in past test experiments. The HBD efficiency for electron identification of the simulation quite differs from that of past test experiments. Here, we use the efficiency of the simulation and the number of J/ψ is scaled to one of the test experiments in Sec. 3.2. The simulation implemented the detector performance archived at the pilot will be completed before our TDR submission. In this section, "the E16 experiment" means the data taking of the E16 RUN1 without any modification and "this experiment" means the data taking with the setup described at Sec. 2.1, respectively.

The reconstruction capability of J/ψ with the E16 RUN1 spectrometer was studied. Electron tracks were reconstructed using hit information of the SSD and the GTR. Associated hits at the HBD and the LG with the reconstructed track were required to identify electrons. The HBD hit corresponding to the track with (number of photo-electron)$\geq$4 was required for each track. The energy deposit at the LG was defined as the sum of the energy deposit at 5 LG blocks which were the LG block corresponding to the track and the four quarters of it. For the LG cut condition, (energy deposit)$>$0.9 GeV/c^2 or (energy deposit)/(momentum)$>$0.3 were required for each track. Since this simulation study was performed to evaluate the feasibility of the

measurement, the analysis cut for the electron identification was somewhat loose.

The tracking analysis performed for this experiment is the same as that for the E16 RUN1 setup. In this simulation study, a single J/ψ was embedded in a p+Pb collision event generated by nuclear cascade code JAM[60]. In addition, random hits of 5 kHz/mm^2 were added to the innermost GTR and the SSD as a beamhalo contribution. The number of the random hits were based on the initial assumption of the E16 proposal, not the pilot run. The realistic evaluation based on the pilot run will be performed before the TDR submission. Figure 5 shows the simulated invariant mass distribution of the reconstructed J/ψ. In Fig. 5, a track finding was also performed. Panel (a) shows the mass distribution in the case of the E16 RUN1 and panel (b) shows one in the case of this experiment, respectively. Fig. 5 demonstrates J/ψ can be reconstructed with a good resolution by using the spectrometer even if the target is moved by 26 cm upstream.

The reconstruction efficiency of J/ψ was also evaluated by using the above embedding simulation. The evaluated reconstitution efficiency includes the track finding efficiency. The reconstitution efficiency also included the trigger efficiency, that is, the above tracking analysis was performed for the events satisfy an assumed trigger condition. For the E16 trigger condition, we assumed (energy deposit)>0.4 GeV in a single LG and (number of photo-electron)$\geq$6 in a HBD hit for each electron candidate. A large opening angle, which was determined by the distance between the two HBD trigger segments, was also required for the trigger condition. (direct distance)>7 segments and (vertical distance)$\geq$1 segments were required for the two HBD segments of the candidate pair. For this experiment, the threshold for the LG hit was assumed to be 0.7 GeV to reduce the effect of increasing γ conversion on the trigger rate due to the Pb target use. The left panel in Figure 6 shows the evaluated reconstruction efficiency

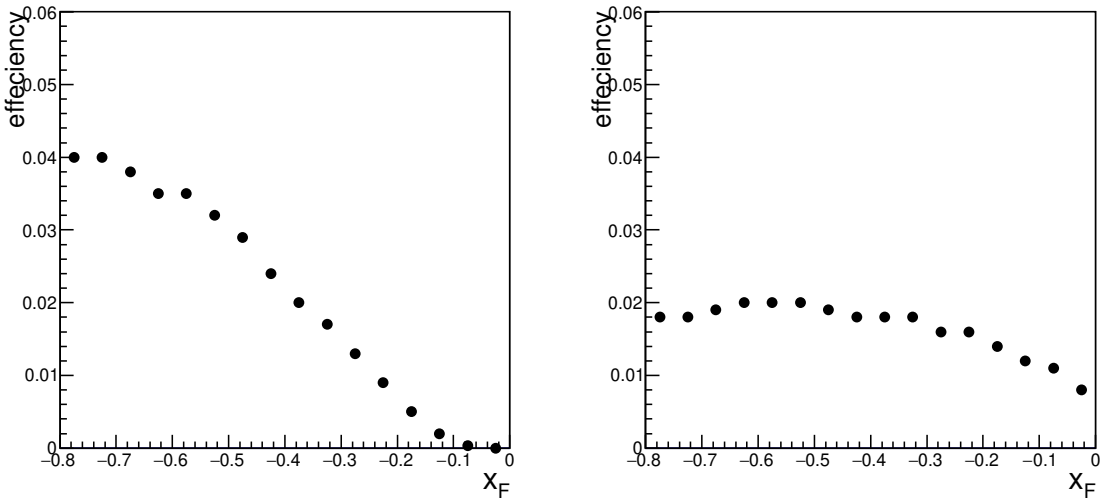

Figure 6: The evaluated reconstruction efficiency of J/ψ as a function of x_F: (left) the E16 RUN1 and (right) this experiment.

of J/ψ as a function of x_F for the E16 setup. Although the efficiency is quite well at large negative x_F, most of J/ψ at $x_F > -0.2$ cannot be reconstructed. The right panel in Fig. 6 shows the evaluated reconstruction efficiency of J/ψ for this experiment. The reconstruction efficiency in this experiment is higher than one in the E16 experiment at $x_F > -0.3$. J/ψ at $x_F \sim 0$ can be reconstructed.

3.2 Expected Experimental Result

Table 3: Summary of the parameters used to normalize the statistics.

	E16	this experiment
beam intensity	1×10^{10} ppp	1×10^{10} ppp
beamtime	1680 hours (70 days)	150 hours (50 days)
target	400 μm C, 160 μm Cu 100 μm Ti	400 μm C, 200 μm Pb 100 μm Ti
branching ratio (J/$\psi \to ee$)	5.97%	5.97%
DAQ live time	55%	60%
HBD efficiency(eID)	63%(single)	63%(single)
S/B	5/1	5/1

The J/ψ cross section via the hard process was evaluated by using leading order (LO) perturbative QCD (pQCD) and the color evaporation model (CEM)[51]. The J/ψ cross section via the soft process due to the intrinsic charm was evaluated similarly as Ref.[8, 55]. The details of this calculation are given in the appendix. The cross section and the suppression pattern of J/ψ used are shown in Figure 9 and Figure 12, respectively. By using the following conditions for both of the above J/ψ cross section, the expected results of combining the E16 RUN1 with this experiment were estimated. The reconstruction efficiency is shown in Fig. 6. The efficiency for DAQ live time was assumed to be 55% and 60% for the E16 and this experiment, respectively. The 100 μm Ti vacuum window was also treated as the nuclear target, hence, the statistics of J/ψ from the vacuum window were considered. The signal to background ratio of the J/ψ yield was assumed to be 5/1. As described at Sec. 3.1, the HBD efficiency for the electron identification of the performed simulation is quite larger than that of the past test experiment. We assumed the HBD efficiency of 63% for a single track as similar to the E16 RUN0 proposal[40]. The statistics were normalized to the 1680 hours (70 days) for the E16 and the 1200 hours (50 days) for this experiment, respectively. The parameters used to normalize the statistics are summarized in Table. 3.

Figure 7 shows the J/ψ yield per nucleon normalized by that of the C target as a function of the normalized nucleon number (A/12). Each panel shows the result of x_F region shown in Fig. 7. In this calculation, EPS09 was used for the nuclear modification and P_{IC} was 0.3% in the model parameters in appendix. Each normalized yield was fitted by a function of $(A/12)^{\alpha-1}$ and the results were also shown in Fig. 7. Figure 8 shows the evaluated α as a function of x_F. In the figure, the red smooth

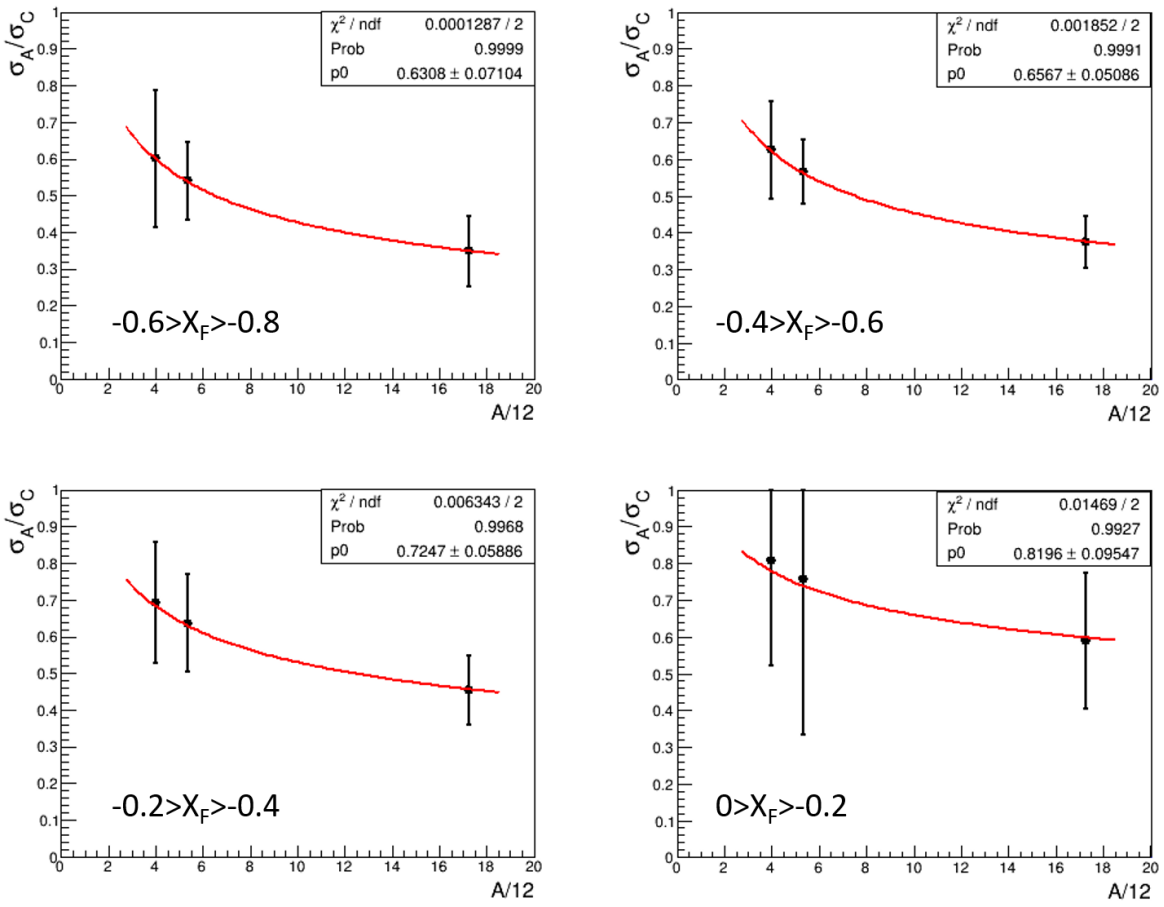

Figure 7: J/ψ yield per nucleon normalized by that of the C target as a function of the normalized nucleon number (A/12). Each panel shows the result of x_F region shown in this figure.

line shows the model calculation with $P_{IC} = 0.3\%$ and the blue dashed line shows one without the intrinsic charm. When the expected result is compared with the calculation without the intrinsic charm, χ^2/ndf is 25.4/4. Even for a relatively small P_{IC}, it is shown that it is possible to confirm the tendency of x_F dependence due to the effect of the intrinsic charm. In Fig. 8, the absolute value in the case without the intrinsic charm depends on the J/ψ absorption cross section (σ_{abs}). In this model calculation, σ_{abs} = 10 mb is assumed based on extrapolation of various results summarized at Ref.[58]. In order to reject the case without the intrinsic charm for any σ_{abs}, the E16 RUN2 and additional beamtime with the proposed setup are necessary. Nevertheless, the proposed experiment will be the valuable measurement of backward J/ψ production at low energy region. It gives the first study to confirm the effect of the intrinsic via backward J/ψ production.

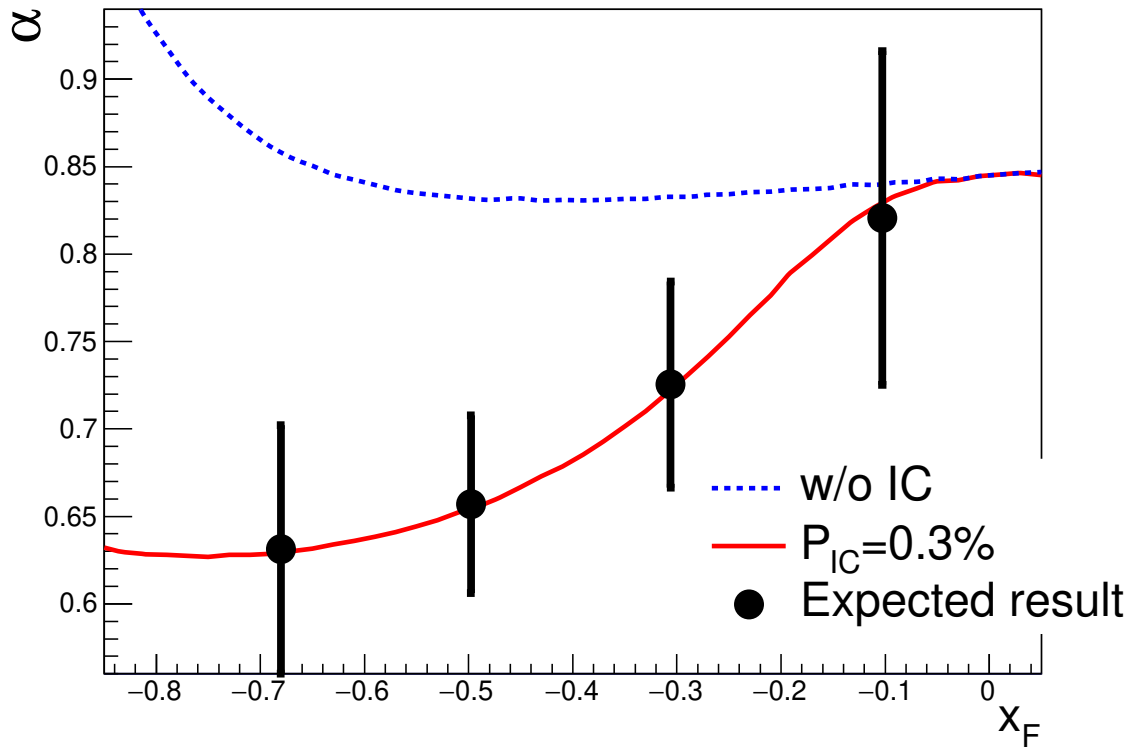

Figure 8: The expected experimental result (black circles) in t he case of nPDF=DSSZ and $P_{IC} = 0.3\%$, and the model calculations without IC (black dashed line) and with $P_{IC} = 0.3\%$ (blue smooth line).

4 Schedule and Costs

This experiment can be started after the E16 RUN1, since there are no development elements in terms of hardware. A part of data will be collected with the E16 run without any modification.

It costs about 10-million Yen to add new targets and to optimize data collection. The costs have been already secured by Kakenhi-B. About 10-million Yen is necessary additionally as the cost of CF4 gas for 50 days running.

A Model calculation of J/ψ yield

Estimation of the J/ψ suppression pattern in hadron-nucleus collisions is necessary to evaluate a quantitative sensitivity of the backward J/ψ measurement to search the intrinsic charm. The J/ψ yield in proton-nucleus collisions is also influenced by known nuclear effects, such as nuclear parton distribution and J/ψ absorption in nucleus, besides the intrinsic charm and the energy loss discussed in Sec. 1.2. A model calculation was performed to evaluate the sensitivity for the intrinsic charm in consideration of such nuclear effects. The model in this study considered the following processes and effects: the hard process and the soft process due to the intrinsic charm as the J/ψ production mechanisms, nuclear parton distribution function (nPDF) as the initial state effect, and the energy of the $c\bar{c}$ color octet and the J/ψ absorption in nucleus as the final state effects.

The J/ψ cross section via the hard process was evaluated by using leading order (LO) perturbative QCD (pQCD) and the color evaporation model (CEM)[51]. In the CEM, J/ψ production is treated identically to open charm production, except that the invariant mass of the $c\bar{c}$ pair is required to be less than the open charm threshold ($2m_D = 3.74\mathrm{GeV/c^2}$). Hence, the cross section of J/ψ is proportional to the integral value of the $c\bar{c}$ cross section over the pair mass from the $c\bar{c}$ production threshold ($2m_c$) to $2m_D$.

$$\frac{d\sigma_{\mathrm{J}/\psi}}{dx_F} = F_{\mathrm{J}/\psi} \int_{4m_c^2}^{4m_D^2} dm^2 \frac{d\sigma_{c\bar{c}}}{dx_F dm^2} \tag{1}$$

where, $F_{\mathrm{J}/\psi}$ is the fraction of the $c\bar{c}$ cross section leading to J/ψ production. In the CEM, $F_{\mathrm{J}/\psi}$ is a constant determined in comparison with the experimental results. The CEM has succeeded to reproduce many features of J/ψ production[52]. The cross section of the $c\bar{c}$ pair, $d\sigma_{c\bar{c}}/(dx_F dm^2)$, was calculated by the QCD factorization theorem and the LO pQCD (See Ref.[8, 53] for details). According to Ref.[53], m_c was 1.5 GeV/c^2 and $F_{\mathrm{J}/\psi}$ was 0.17 in this study, respectively. The factorization and renormalization scale parameters were $2m_c$. We used CTEQ5L for the parton distribution of the nucleon[54]. Figure 9(a) shows the J/ψ cross section as a function of x_F calculated by the LO pQCD and the CEM in pp collisions at 30 GeV.

The J/ψ cross section via the soft process due to the intrinsic charm was evaluated similarly as Ref.[8, 55]. The probability distribution of the intrinsic charm state ($|uudc\bar{c}\rangle$ or $|uddc\bar{c}\rangle$) in a nucleon was assumed as follows[1, 2].

$$\frac{dP_{IC}}{dx_1 \cdot \cdot dx_5} = N_5 \frac{\delta\left(1 - \sum_{i=1}^{5} x_i\right)}{\left(m_p^2 - \sum_{i=1}^{5} (\hat{m}_i^2/x_i)\right)^2} \tag{2}$$

where, N_5 is a normalization factor for P_{IC} and $\hat{m}_i$ is an average traverse mass ($\sqrt{m_i^2 + < k_T^2 >}$). We assumed $\hat{m}$ of the light quark was 0.45 GeV/c^2 and $\hat{m}$ of the charm quark was 2.25 GeV/c^2 respectively since $m_c = 1.5$ GeV/c^2 was used in pQCD and $< k_T^2 > \propto m_i^2$ was expected. N_5 was left as the free parameter to adjust P_{IC}. The cross section of charm production via the intrinsic charm ($\sigma_{c\bar{c}}^{IC}$) is related to P_{IC} and the inelastic cross

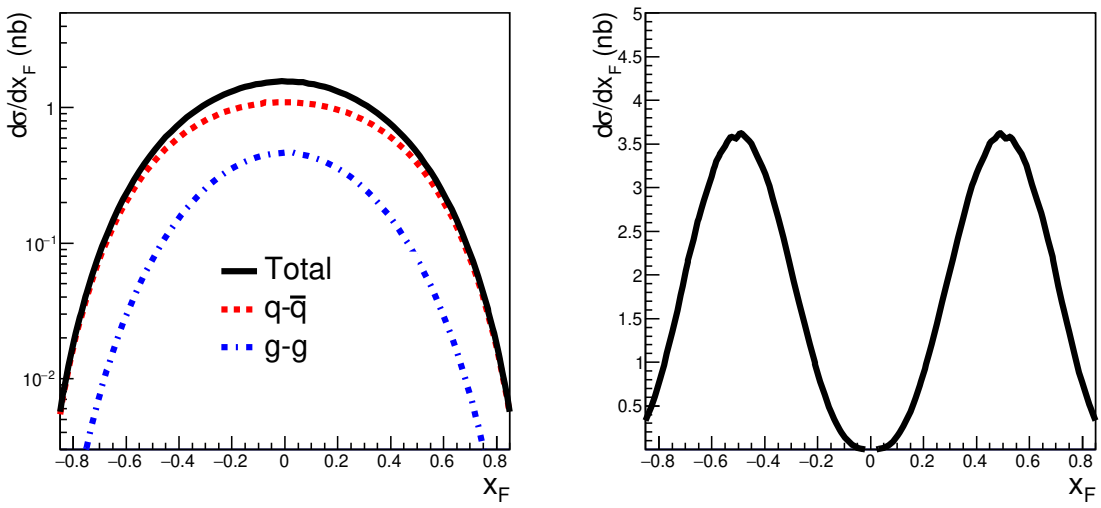

Figure 9: The calculated J/ψ cross section as a function of x_F in pp collisions at 30 GeV. (Left) the hard process calculated by the LO pQCD and the CEM (red dashed line:$q-\bar{q}$ contribution, blue dotted line:$g-g$ contribution, black solid line:total yield). (Right) the soft process originating from the intrinsic charm in the case of $P_{IC} = 0.3\%$.

section (σ^{inel}) as follows.

$$\sigma_{c\bar{c}}^{IC} = P_{IC}\sigma^{inel}\frac{\mu^2}{4\hat{m}_c^2} \tag{3}$$

where, $\mu^2/4\hat{m}_c^2$ is the soft interaction factor to break the intrinsic charm state. $\mu^2 = 0.1$ GeV^2 was used according to Ref.[8]. (it was determined in comparison with the J/ψ cross section measured at NA3.) The J/ψ cross section ($\sigma_{\mathrm{J}/\psi}^{IC}$) is related to the $c\bar{c}$ cross section via the intrinsic charm as in the CEM. Hence,

$$\frac{d\sigma_{\mathrm{J}/\psi}^{IC}}{dx_F} = F_{\mathrm{J}/\psi}^{IC}\sigma^{inel}\frac{\mu^2}{4\hat{m}_c^2}\int\prod_{i=1}^{5}dx_i\int_{4m_c^2}^{4m_D^2}dm^2\frac{dP_{IC}}{dx_1\cdot\cdot dx_5 dm^2}\delta(x_F - x_c - x_{\bar{c}}) \tag{4}$$

where, $F_{\mathrm{J}/\psi}^{IC}$ is the fraction of the $c\bar{c}$ cross section via the intrinsic charm leading to J/ψ production. $F_{\mathrm{J}/\psi}^{IC} = 0.17 \times 1/4$ was used, where 0.17 was common with the hard process and 1/4 was *"the flavor suppression factor"* relating with the intrinsic charm process[55]. Gauss distribution was assumed for k_T in this integral. Fig. 9(b) shows the calculated J/ψ cross section via the soft process as a function of x_F in pp collisions at 30 GeV in the case of $P_{IC} = 0.3\%$. It is confirmed that the contribution from the soft process is concentrated at the large $|x_F|$ region. The nuclear dependence of this soft process is $A^{2/3}$.

We used two results of the latest nPDF global analyses, called "EPS09"[56] and "DSSZ"[57], as nPDFs in this model calculation. Figure 10 shows the DSSZ and EPS09 nuclear effects to bound-proton PDFs in Pb as a function of x at the initial scales $Q^2 = 9$GeV^2. Although there is not a major difference between DSSZ and EPS09

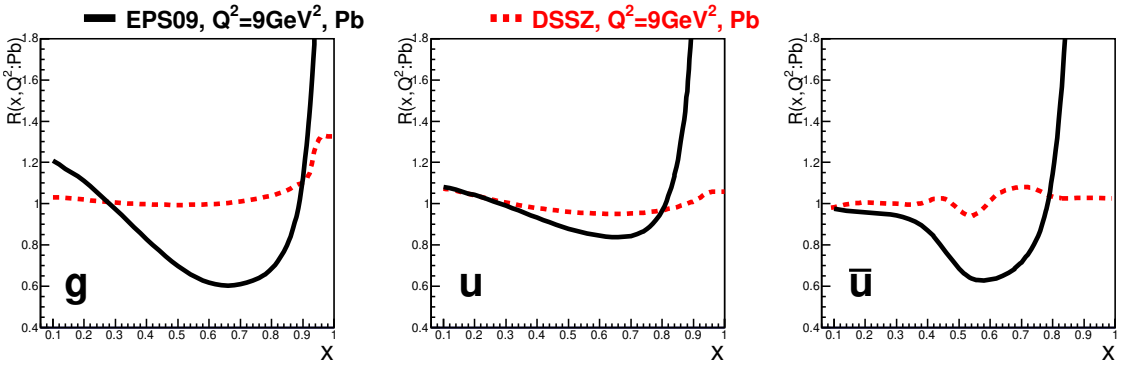

Figure 10: The DSSZ and EPS09 nuclear effects to bound-proton PDFs in Pb as a function of x at the initial scales $Q^2 = 9\text{GeV}^2$ for gluon (left), u quark (middle), and $\bar{u}$ quark (right). Black solid lines represent the EPS09 and red dashed lines represent the DSSZ, respectively.

for the input experimental results as constraints for nPDFs, these two nPDFs differ at EMC region as shown at Fig. 10. The essential difference between the two analyses is that the DSSZ analysis uses the nuclear fragmentation functions[57]. The two analyses were used, and the results were compared to consider the uncertainty of nPDFs.

The path length of the $c\bar{c}$ color octet in the nuclear matter was calculated assuming $\tau_\psi = 0.3$ fm, which was evaluated based on the uncertainty principle[44]. The $c\bar{c}$ color octet was produced uniformly in the nucleus, and then the path length in the nuclear matter was calculated as a function of x_F. Figure 11 shows the mean path length of the color octet as a function of x_F in the case when the targets are C, Cu, and Pb. Most of the color octet change to the color singlet in the nuclear matter even if the target is C. Therefore, the mean fight length of the color octet is almost the same from C to Pb, leading that the energy loss is also the same from C to Pb. The energy loss of the color octet consequently does not make the nuclear dependence if C is used as the reference. In the above reason, the energy loss of the color octet was neglected in this model calculation.

The path length of J/ψ in the nuclear matter was calculated similarly as the $c\bar{c}$ color octet. Then, the survival probability of J/ψ in nucleus was calculated according to $\exp(-L_\psi \rho \sigma_{abs})$, where L_ψ is the path length of J/ψ in the nuclear matter, ρ (0.17 fm^{-3}) is the nuclear density, and σ_{abs} is the J/ψ absorption cross section, respectively. $\sigma_{abs} = 10$ mb was assumed in this study based on extrapolation of various results summarized in Ref.[58]. Although this assumption is determined by rough extrapolation, the uncertainty of this parameter does not change much the shape of the J/ψ suppression pattern.

The J/ψ suppression pattern was evaluated based on the above processes for 30 GeV protons incident on the nucleus. Figure 12 shows the evaluated J/ψ suppression degree in terms of α as a function of x_F. The left panel shows the result in the case of nPDF=EPS09 and the right panel shows one in the case of nPDF=DSSZ, respectively. P_{IC} is varied from 0% to 1.0% in Fig. 12. While α at $x_F \sim 0$ does not depend on P_{IC},

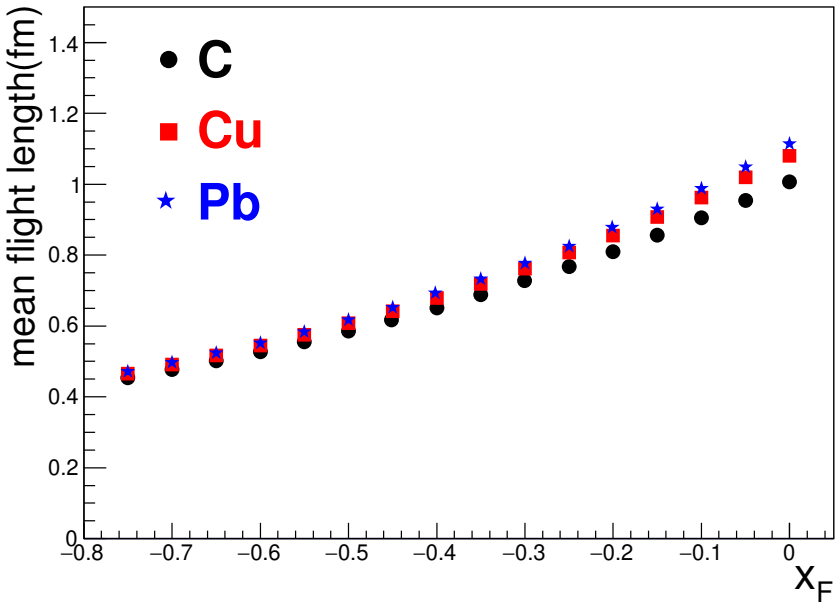

Figure 11: The mean path length of the $c\bar{c}$ color octet in the nuclear matter as a function of x_F when the targets are C (black circles), Cu (red squares), and Pb (blue stars).

α at large negative x_F degrees clearly depending on P_{IC} in both nPDF. The deviation of α at $x_F \sim 0$ from 1 is the result of the J/ψ nuclear absorption and nPDF. The effect of the intrinsic charm appears as the deviation of α at large negative x_F from α at $x_F \sim 0$. While $P_{IC} < 0.2\%$ at the 5σ level is the most negative result of the current study, the effect of the intrinsic charm can be clearly seen at Fig. 12 even in the case of $P_{IC} = 0.05\%$. The sensitivity of backward J/ψ production at 30 GeV to the intrinsic charm is fairly well.

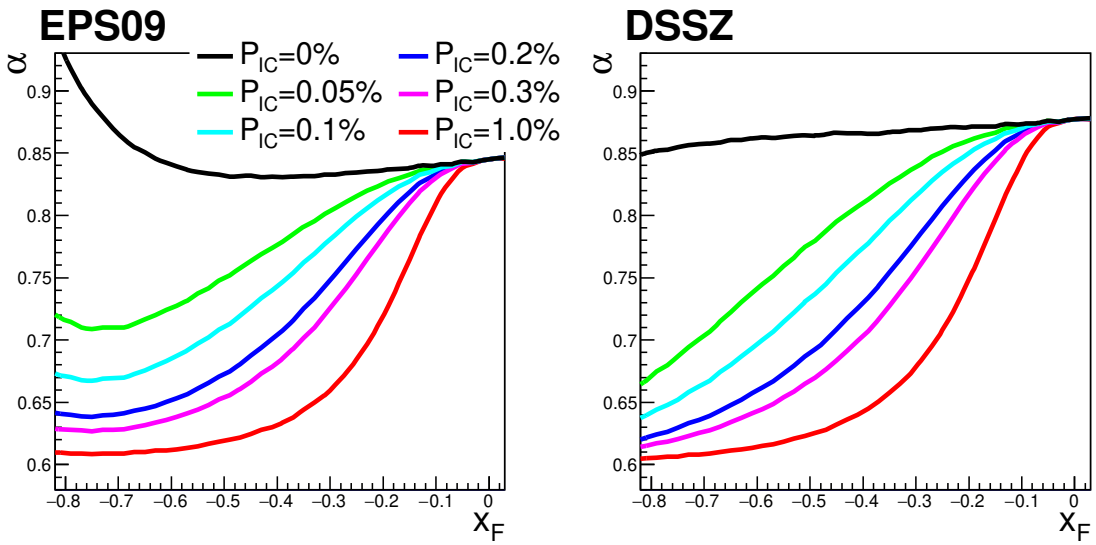

Figure 12: The evaluated J/ψ suppression degree (α) as a function of x_F with various P_{IC} in the case of nPDF=EPS09 (left) and nPDF=DSSZ (right).

References

[1] S. J. Brodsky, P. Hoyer, C. Peterson, and N. Skai, Phys. Lett. **B 93** 451 (1980).

[2] S. J. Brodsky, C. Peterson, and N. Skai, Phys. Rev. D **23** 2745 (1981).

[3] J. Badier *et al.*, Z. Phys. **C20** 101 (1983).

[4] M. J. Leitch *et al.*, Phys. Rev. Lett **84** 3256 (2000).

[5] D. M. Alde *et al.*, Phys. Rev. Lett **66** 133 (1991).

[6] I. Abt *et al.*, Eur. Phys. J. **C60** 525 (2009).

[7] R. Arnaldi *et al.*, Phys. Lett. **B706** 263 (2012).

[8] R. Vogt, Phys. Rev. C **61** 035203 (2000).

[9] E. M. Aitala *et al.*, Phys. Lett. **B371** 157 (1996).

[10] P. Chauvat *et al.*, Phys. Lett. **B199** 304 (1987).

[11] M. I. Adamovich, *et al.*, Eur. Phys. J.**C8** 593 (1999).

[12] F. G. Garcia *et al.*, Phys. Lett. **B528** 49 (2002).

[13] T. Gutierrez and R. Vogt, Nucl. Phys. **B539** 189 (1999).

[14] Particle Data Group. Chin. Phys. C **40**, 100001 (2016).

[15] S. J. Brodsky and M. Karliner, Phys. Rev. Lett **78** 4682 (1997).

[16] M. Mattson *et al.*, Phys. Rev. Lett. **89** 112001 (2002).

[17] J. Badier *et al.*, Phys. Lett. **B158** 457 (1985).

[18] R. Vogt and S. J. Brodsky, Phys. Lett. **B349** 569 (1995).

[19] S. Koshkarev and V. Anikeev, Phys. Lett. **B765** 171 (2017).

[20] S. J. Brodsky, B. Kopeliovich, I. Schmidt, and J. Soffer, Phys. Rev. D **73** 113005 (2006).

[21] T. Boettcher, P. Ilten, and M. Williams, Phys. Rev. D **93** 074008 (2016).

[22] J. Pumplin, H. L. Lai and W. K. Tung, Phys. Rev. D **75** 054029 (2007).

[23] J. R. Ellis, K. A. Olive, and C. Savage, Phys. Rev. D **77** 065026 (2008).

[24] J. Giedt, A. W. Thomas, and R. D. Young, Phys. Rev. Lett **103** 201802 (2009).

[25] T. Hatsuda and T. Kunihiro, Nucl. Phys. **B387** 715 (1992).

[26] A. Abdel-Rehim *et al.*, Phys. Rev. Lett **116** 252001 (2016).

[27] W. Freeman and D. Toussaint, Phys. Rev. D **88** 054503 (2013).

[28] M. Gong *et al.*, Phys. Rev. D **88** 014503 (2013).

[29] J. J. Aubert *et al.*, Nucl. Phys. **B213** 31 (1983).

[30] E. Hoofmann and R. Moore, Z. Phys. **C20** 71 (1983).

[31] B. Harris, J. Smith, and R. Vogt, Nucl. Phys.**B461** 181 (1996).

[32] F. M. Steffens, W. Melnitchouk, and A. W. Thomas, Eur. Phys. J.**C11** 673 (1999).

[33] J. Pumplin, H. L. Lai, and W. K. Tung, Phys. Rev. D **75** 054029 (2007).

[34] P. M. Nadolsky *et al.* , Phys. Rev. D **78** 012004 (2008).

[35] S. Dulat *et al.* , Phys. Rev. D **89** 073004 (2014).

[36] P. Jimenez-Delgado, T. J. Hobbs, J. T. Londergan, and W. Melnitchouk, Phys. Rev. Lett **114** 082002 (2015).

[37] H. Abramowicz *et al.*, Eur. Phys. J.**C73** 2311 (2013).

[38] S. J. Brodsky *et al.*, Adv. High Energy Phys.**2015** 231547 (2015).

[39] S. Yokkaichi, Lect. Notes. Phys.**C781** 161 (2009).

[40] S. Yokkaichi *et al.*, J-PARC Proposal,
http://j-parc.jp/researcher/Hadron/en/pac_1707/pdf/E16_2017-10.pdf

[41] P. Hoyer, M. Vanttinen and U. Sukhatme, Phys. Lett. **B246** 217 (1990).

[42] M. A. Vasiliev *et al.*, Phys. Rev. Lett **83** 2304 (1999).

[43] S. J. Brodsky and P. Hoyer, Phys. Rev. Lett **63** 1566 (1989).

[44] D. Kharzeev and H. Satz, Z. Phys. **C60** 389 (1993).

[45] F. Arleo, P. B. Gossiaux, T. Gousset, and J. Aichelin, Phys. Rev. C **61** 054906 (2000).

[46] F. Arleo and S. Peigné, Phys. Rev. Lett **109** 122301 (2012).

[47] R. Vogt, S. J. Brodsky and P. Hoyer, Nucl. Phys. **B360** 67 (1991).

[48] Y. Komatsu *et al.*, Nucl. Instrum. Meth. A **732** 241 (2013).

[49] K. Aoki *et al.*, Nucl. Instrum. Meth. A **628** 300 (2011).

[50] K. Kanno *et al.*, Nucl. Instrum. Meth. A **819** 20 (2016).

[51] H. Fritzsch, Phys. Lett. **B67** 217 (1977).

[52] G. A. Schuler and R. Vogt, Phys. Lett. **B387** 181 (1996).

[53] J. C. Peng, D. M. Jansen and Y. C. Chen, Phys. Lett. **B344** 1 (1995).

[54] H. L. Lai *et al.*, Eur. Phys. J. **C12** 375 (2000).

[55] R. Vogt and S. J. Brodsky, Phys. Lett. **B349** 569 (1995).

[56] E. J. Eskola, H. Paukkunen and C. A. Salgado, J. High. Energy. Phys **04** 065 (2009).

[57] D. de Florian, R. Sassot, P. Zurita and M. Stratmann, Phys. Rev. D **85** 074028 (2012).

[58] C. Lourenco, R. Vogt and H. K. Woehri, J. High. Energy. Phys **02** 014 (2009).

[59] S. Agostinelli *et al.*, Nucl. Instrum. Meth. A **506** 250 (2003).

[60] Y. Nara *et al.*, Phys. Rev. C **61** 024901 (2000).

[61] Y. Morino *et al.*, J-PARC LOI, http://j-parc.jp/researcher/Hadron/en/pac_1801/pdf/LoI_2018_6.pdf